Supplementary Information

Micro- and Nanoscale $CaCO_3$ Carriers for Localized Melanoma Therapy: Impact of 'Cold' Labeling on Drug Loading, Release, and *In Vivo* Performance

Darya R. Akhmetova[1,2], Vladislava A. Rusakova[1], Denis A. Matveev[1], Darya P. Toloknyannikova[3], Jiaxian Cai[4,5], Bochang Feng[4,5], Menghua Xiong[4,5,6], Sergei A. Shipilovskikh[1,2], Dong Luo[4,5,7,*], Alexander S. Timin[1,*]

[1]Laboratory of nano- and microencapsulation of biologically active compounds, Peter The Great St. Petersburg Polytechnic University, 195251, St. Petersburg, Russian Federation

[2]International Research and Educational Center for Physics of Nanostructures, ITMO University, 194021, St. Petersburg, Russian Federation

[3]Saint Petersburg State Chemical Pharmaceutical University, 197022, St. Petersburg, Russian Federation

[4]School of Biomedical Sciences and Engineering, South China University of Technology, Guangzhou International Campus, Guangzhou, 511442, P. R. China

[5]National Engineering Research Centre for Tissue Restoration and Reconstruction, South China University of Technology, Guangzhou, 510006, P. R. China

[6]Key Laboratory of Biomedical Materials of the Ministry of Education, South China University of Technology, Guangzhou 510006, P. R. China

[7]Guangdong Province Key Laboratory of Biomedical Engineering, South China University of Technology, Guangzhou 510006, P. R. China

*Correspondence to Dr. Dong Luo (luodong09@scut.edu.cn) and Dr. Alexander S. Timin (a_timin@mail.ru, timin_as@spbstu.ru).

Table of contents

1. Materials

1.1. For synthesis of compound 5 (2AT)

All the air-sensitive reactions were carried out under nitrogen atmosphere in standard Schlenk flasks. All the chemicals were analytical grade and used without further purification. 4′-Methoxyacetophenone (99%), diethyl oxalate (≥ 99%), sodium methoxide (95%), cyclohexanone (≥ 99.0%), sulfur (99.98%), morpholine (≥ 99%), ethyl cyanoacetate (≥ 98%), propionic anhydride (≥ 99%), cyanoacetamide (99%), and potassium *tert*-butoxide (≥ 98%) were purchased from Sigma-Aldrich (Germany). Methanol (MeOH), ethanol (EtOH), and dioxane were dried over activated molecular sieves (3 Å) in Erlenmeyer flasks for two days before use. Chemically pure grade solvents were subjected to additional purification and drying. All other reagents were purchased from various commercial sources and used without additional purification.

1.2. For mCa and nCa synthesis

Calcium chloride dihydrate ($CaCl_2 \times 2H_2O$), anhydrous sodium carbonate (Na_2CO_3), poly(acrylic acid) (PAA, №32667) were purchased from SigmaAldrich (Germany) and used without further purification. Purified water with specific resistivity higher than 18.2 MΩ cm^{-1} from a three-stage Milli-Q Plus 185 purification system was used. Sodium chloride (NaCl) was purchased from ITW Reagents Panreac (Spain).

1.3. For mCa and nCa modifications

Sulfo-cyanine 5 NHS ester (Cy5, M_w=777.95) was purchased from Lumiprobe (Germany). Bovine serum albumin (BSA, M_w=66 kDa) was purchased from Sigma-Aldrich (Germany) and used without further purification.

1.4. For mCa and nCa 'cold' labeling

Barium chloride dihydrate ($BaCl_2 \times 2H_2O$) and anhydrous sodium sulfate (Na_2SO_4) were purchased from Sigma-Aldrich (Germany) and used without further purification.

1.5. For in vitro experiments

Alpha Minimum Essential Medium (Alpha-MEM) was purchased from Biolot (Russia). Phosphate-buffered saline (PBS) was purchased from Lonza (Switzerland). Adult bovine serum (ABS) was purchased from Capricorn Scientific (Germany). The trypsin solution was purchased from Biolot (Russia). Doxorubicin-LENS (2 mg/mL) was purchased from Veroharm (Russia). TWEEN80, FITC-phalloidin and resazurin sodium salt (M_w=251.17) were purchased from Sigma-Aldrich (Germany).

1.6. For in vivo experiments

C57BL/6 mice (female, age 8 weeks, weight 18-22 g) were purchased from Rappolovo (Russia). Phosphate-buffered saline (PBS) was purchased from Lonza (Switzerland).

1.7. For histological analysis

Formaldehyde, paraffin, 1% hydrochloric acid solution, methanol, potassium hexacyanoferrate (II) trihydrate, and PBS (phosphate buffered saline) were purchased from Thermo Fisher Scientific (USA). IsoPREP ready-to-use solution and HISTOMIX paraffin medium were received from Biovitrum, Russia. Ehrlich's hematoxylin was purchased from Labiko (Russia). Eosin Y (M_w=647.89) was purchased from Sigma-Aldrich (Germany). Glycergel mounting medium was purchased from Agilent Dako (USA).

2. Synthetic procedures

2.1 Synthesis of compound 5 (2AT)

2.1.1. Synthesis of compounds 1-5

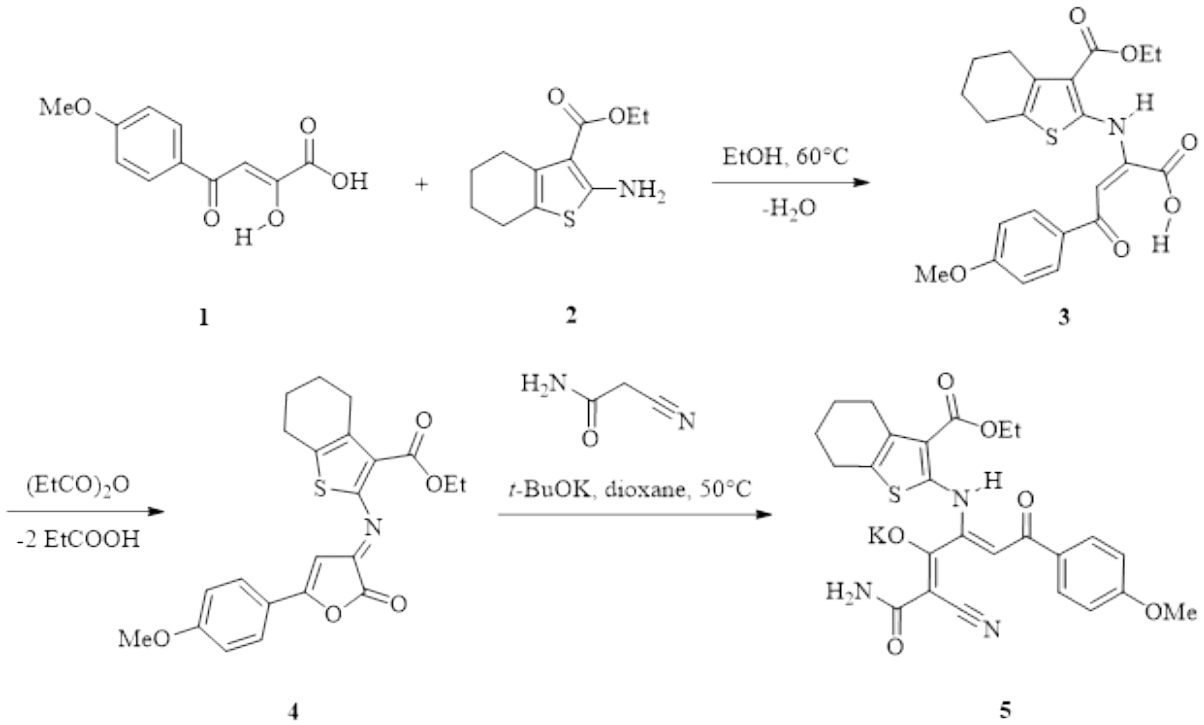

Fig. S1 Scheme of multistep synthesis of compound 5 (2AT) [1].

2.1.2. Procedure for the synthesis of compound 1

(*Z*)-2-hydroxy-4-(4-methoxyphenyl)-4-oxobut-2-enoic acid 1 was synthesized according to known procedures [2]. The physicochemical data of the obtained compound 1 corresponds to the previously described.

(Z)-2-hydroxy-4-(4-methoxyphenyl)-4-oxobut-2-enoic acid 1. White crystals; 39.55 g, 88% yield; m.p. 160 - 162°C. ^{1}H NMR ($CDCl_3$, 400 MHz): δ, 8.02 (m, 2H), 7.12 (s, 1H), 7.02 (m, 2H), 3.93 (s, 3H). ^{13}C NMR ($CDCl_3$, 100 MHz): δ, 164.8, 161.9, 132.1, 130.4, 125.6, 114.5, 94.4, 55.6.

2.1.3. Procedure for the synthesis of compound 2

Ethyl 2-amino-4,5,6,7-tetrahydrobenzo[*b*]thiophene-3-carboxylate 2 was synthesized according to known procedures [2]. The physicochemical data of the obtained compound 2 correspond to the previously described.

Ethyl 2-amino-4,5,6,7-tetrahydrobenzo[b]thiophene-3-carboxylate 2. Yellow crystals; 19.15 g, 85% yield; m.p. 119 - 120°C. ^{1}H NMR ($CDCl_3$, 400 MHz): δ, 5.93 (s, 2H), 4.28 (q, *J* = 7.1 Hz, 2H), 2.73 (m, 2H), 2.52 (m, 2H), 1.79 (m, 4H), 1.36 (t, *J* = 7.1 Hz, 3H). ^{13}C NMR ($CDCl_3$, 100 MHz): δ, 166.1, 161.6, 132.5, 117.7, 105.9, 59.3, 26.9, 24.5, 23.3, 22.8, 14.4.

2.1.4. Procedure for the synthesis of compound 3

A solution of the (*Z*)-2-hydroxy-4-(4-methoxyphenyl)-4-oxobut-2-enoic acid 1 (2.22 g, 0.01 mol) in ethanol (10 ml) was added to a solution of ethyl 2-amino-4,5,6,7-tetrahydrobenzo[*b*]thiophene-3-carboxylate 2 (2.25 g, 0.01 mol) in ethanol (10 ml). The resulting mixture was heated to 60°C and stirred for 1 hour. After completion of the reaction, the solution was cooled to -27°C, the precipitate was filtered off and recrystallized. The physicochemical data of the obtained compound 3 correspond to the previously described [2].

2-{[3-(Ethoxycarbonyl)-4,5,6,7-tetrahydrobenzo[b]thiophen-2-yl]amino}-4-(4-methoxyphenyl)-4-oxobut-2-enoic acid 3. Red crystals; 3.86 g, 90% yield; m.p. 186 - 187°C (acetonitrile). ^{1}H NMR ($CDCl_3$, 400 MHz): δ, 12.19 (s, 1H), 8.03 (m, 2H), 7.08 (s, 1H), 7.01 (m, 2H), 4.38 (q, *J* = 7.1 Hz, 2H), 3.91 (s, 3H), 2.81 (m, 2H), 2.77 (m, 2H), 1.88 (m, 2H), 1.82 (m, 2H), 1.40 (t, *J* = 7.1 Hz, 3H). ^{13}C NMR ($CDCl_3$, 100 MHz): δ, 187.7, 164.4, 164.3, 162.4, 145.5, 144.5, 134.6, 131.2, 129.6, 128.7, 117.6, 114.3, 96.5, 61.3, 55.7, 26.5, 24.9, 22.7, 22.4, 14.2.

2.1.5. Procedure for the synthesis of compound 4

A solution of compound 3 (3.86 g, 0.009 mol) in propionic anhydride (5 ml) was slowly heated to 140°C and then stirred for 1 h. The precipitate formed after cooling down was filtered off, washed with absolute ether, and recrystallized from anhydrous toluene. The physicochemical data of the obtained compound 4 correspond to the previously described [2].

Ethyl 2-((5-(4-methoxyphenyl)-2-oxofuran-3(2H)-ylidene)amino)-4,5,6,7-tetrahydrobenzo[b]thiophene-3-carboxylate 4. Red crystals; 3.33 g, 90% yield; m.p. 146 - 147°C (toluene). ^{1}H NMR ($CDCl_3$, 400 MHz): δ, 7.80 (m, 2H), 7.00 (m, 2H), 6.77 (s, 1H), 4.38 (q, *J* = 7.1 Hz, 2H), 3.90 (s, 3H), 2.79 (m, 2H), 2.75 (m, 2H), 1.87 (m, 2H), 1.82 (m, 2H), 1.40 (t, *J* = 7.1 Hz, 3H). ^{13}C NMR ($CDCl_3$, 100 MHz): δ, 166.5, 164.1, 163.6, 161.3, 149.7, 146.2, 138.2, 136.0, 131.6, 128.7, 119.5, 114.8, 96.4, 61.2, 55.9, 25.7, 25.2, 22.9, 22.3, 14.3.

2.1.6. Procedure for the synthesis of compound 5 (2AT)

The cyanacetamide (0.42 g, 5 mmol) was added to a solution of compound 4 (2.06 g, 5 mmol) in 75 mL of anhydrous dioxane, then *t*-BuOK (0.56 g, 5 mmol) was added, and the resulting solution was heated to 50°C and stirred for 60 min. After completion of the reaction, the solution was cooled to r.t, the precipitate was filtered off and recrystallized from dioxane.

Potassium 1-amino-2-cyano-4-((3-(ethoxycarbonyl)-4,5,6,7-tetrahydrobenzo[b]thiophen-2-yl)amino)-6-(4-methoxyphenyl)-1,6-dioxohexa-2,4-dien-3-olate 5. Yellow solid; 91% yield; m.p. 201 - 202°C (dioxane). ^{1}H NMR (DMSO-*d6*, 400 MHz): δ, 13.46 (s, 1H), 8.53 (s, 1H), 7.94 (m, 2H), 7.02 (m, 2H), 6.38 (s, 1H), 6.02 (s, 1H), 4.36 (q, *J* = 7.0 Hz, 2H), 3.83 (s, 3H), 2.69 (m, 2H), 2.55 (m, 2H), 1.71 (m, 4H), 1.35 (m, *J* = 7.0 Hz, 3H). ^{13}C NMR (DMSO-*d6*, 100 MHz): δ, 187.8, 179.1, 168.7, 163.4, 162.2, 156.0, 148.7, 131.9, 131.6,

129.4, 125.9, 123.3, 113.8, 112.5, 95.0, 79.7, 60.0, 55.4, 26.1, 24.0, 22.5, 22.3, 14.4.

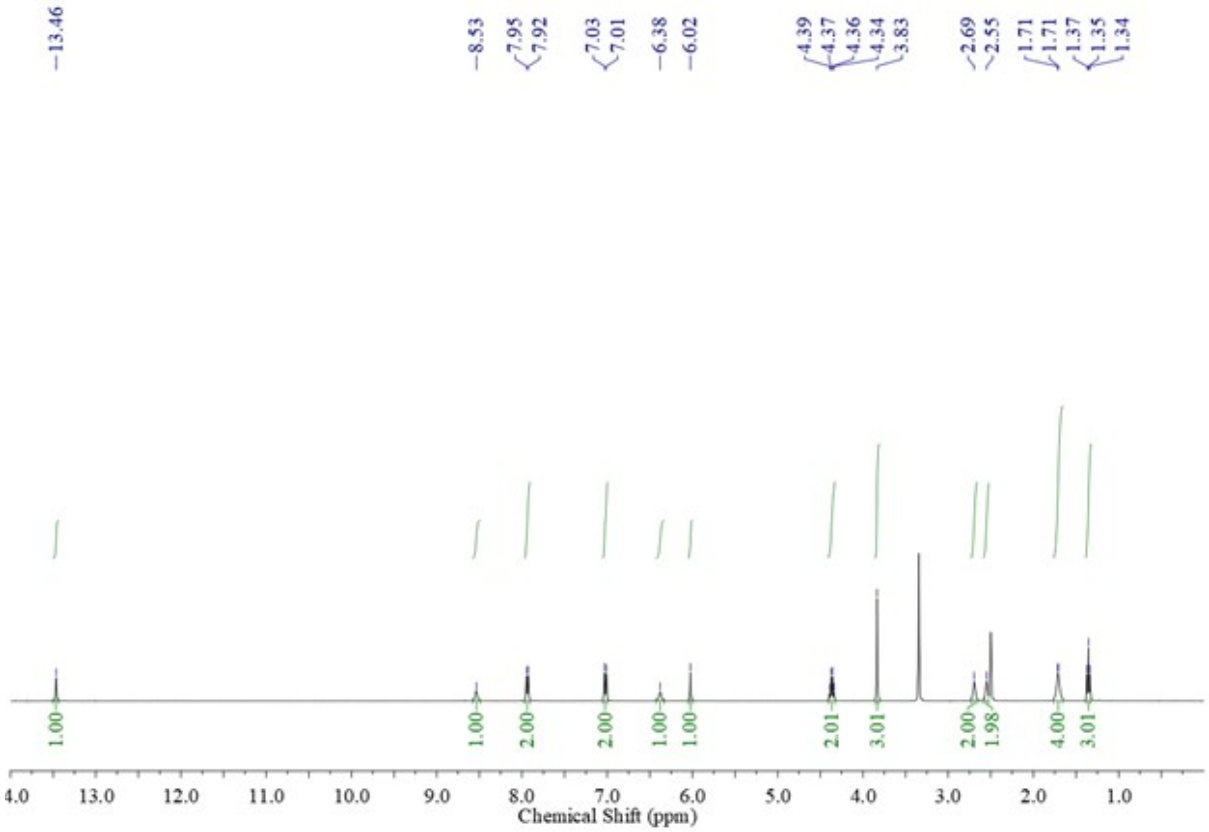

Fig. S2 ^{1}H NMR spectrum of compound 5 (2AT) (DMSO-d_6, 400 MHz).

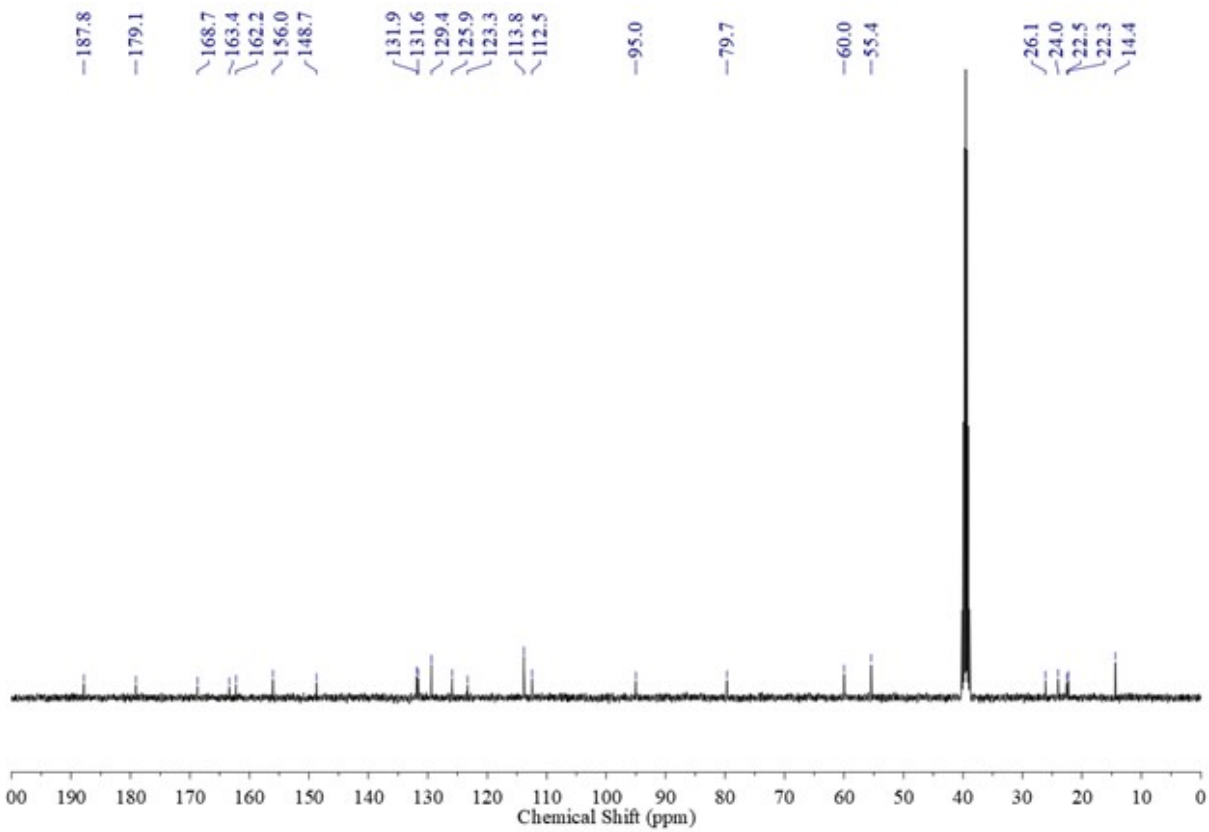

Fig. S3 ^{13}C NMR spectrum of compound 5 (2AT) (DMSO-d_6, 100 MHz)

2.2. Synthesis of mCa/nCa particles

The $CaCO_3$ microparticles (mCa) were synthesized by co-precipitation method. For this, $CaCl_2$ (1 M) aqueous solution and Na_2CO_3 (1 M) aqueous solution were selected for this purpose. 615 μL of both solutions were added to 2.5 mL Milli-Q water and mixed for 30 sec. The resulting suspension was washed 3 times with Milli-Q water and centrifuged on the microspin for 30 sec at 3 500 rpm.

The $CaCO_3$ nanoparticles (nCa) were also synthesized by co-precipitation. For this, 3 mL of aqueous solution polyacrylic acid (PAA, 3 mg/mL) was added to 3 mL of an aqueous solution $CaCl_2$ (0.1 M) and stirred for 1 h. Then, 3 mL of aqueous solution Na_2CO_3 (0.1 M) was added, and the mixture was stirred for 1

h. The final solution was washed 3 times with Milli-Q water and centrifuged for 4 min at 13 400 rpm.

3. Characterization

3.1. Powder X-ray Diffraction (PXRD)

The crystalline phase of mCa and nCa was studied using PXRD. Diffraction patterns were recorded on Bruker D2 Phaser (Germany) diffractometer with a characteristic Cu Kα radiation source (Kα1 λ = 1.54059 Å, angular range 2θ = 5–60°) and a Bragg-Brentano goniometer. The angular resolution during analysis was 0.02 degrees at a scan rate of 2.4 degree/min.

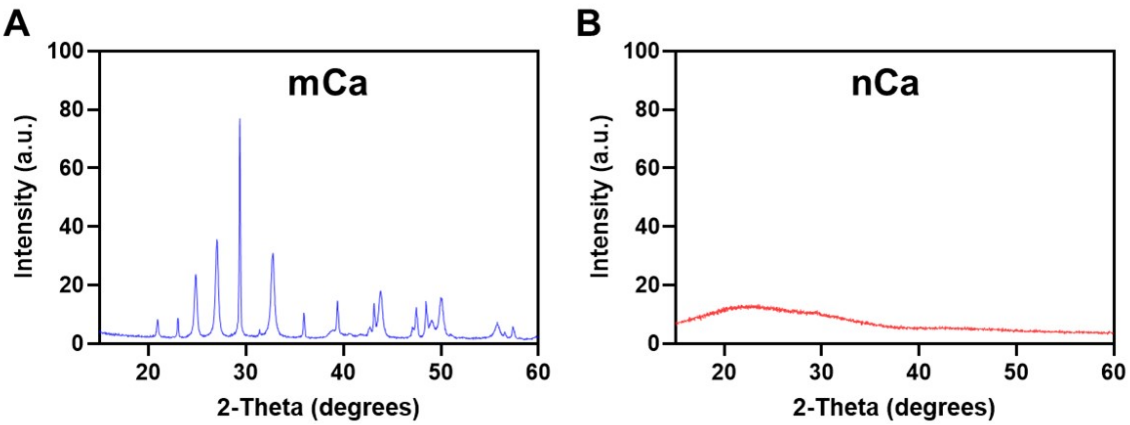

Fig. S4 PXRD patterns of micro- (mCa) and nanoscale (nCa) $CaCO_3$ carriers.

3.2. Scanning electron microscopy

All obtained particle samples were visualized using scanning electron microscopy (SEM - Quanta 200 FEI (Netherlands) and ZEISS Merlin® FE-SEM (Germany)). The accelerating voltages were 30 kV and 20,1 kV respectively. 1 μL of each sample was dropped onto a silicon substrate, dried, and then visualized using SEM.

3.3. Surface area analysis

Surface area of mCa was obtained using the Brunauer-Emmett-Teller (BET) method using BSD-BET400 (Beishide Instrument, China). Specific surface area was calculated using the BET method.

3.4. Transmission electron microscopy

All obtained particle samples were visualized using transmission electron microscopy (TEM - JEOL JEM-1011 (Japan)). 5 μL of each sample was dropped onto a carbon-coated copper grid and then imaged using TEM.

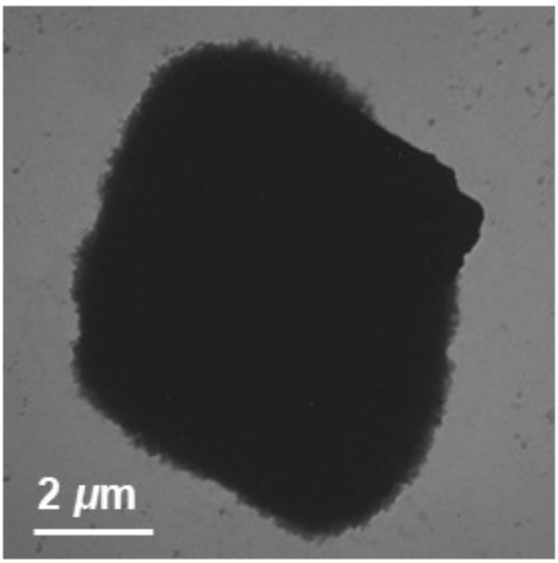

Fig. S5 TEM image of mCa.

3.5. Dynamic laser scattering

Dynamic light scattering (DLS Nano Particle Analyzer - Jinan Winner Particle Instrument Stock Co. (China)) was used to determine the size of mCa, nCa, 'cold' mCa@2AT, and 'cold' nCa@2AT.

3.6. Zeta potential

The ζ-potential (Zetasizer Nano ZS90 analyzer - Malvern Instruments Ltd (United Kingdom)) was used to determine the charge of mCa, nCa.

3.7. Fourier-transform infrared (FTIR) spectroscopy

Fourier transform infrared spectroscopy peaks were obtained with a FTIR Spectrometer (WQF-530A - Beijing Beifen-Ruili Analytical Instrument (China)). Scans were made in the range from 400 to 4000 cm^{-1}, with a resolution of 1 cm^{-1}.

4. 2AT drug loading

4.1. Synthesis of mCa@2AT and nCa@2AT particles

The co-precipitation method was used to prepare mCa@2AT. 100 μL of 2AT (0.5, 1, 2, 5 and 10 mg) were added to 2.4 mL of Milli-Q water. Then 615 μL of aqueous solution of $CaCl_2$ (0.1M) and 615 μL of aqueous solution of Na_2CO_3 (0.1M) were added to the first solution. The resulting suspension was stirred for 30 sec and washed 3 times with Milli-Q water with centrifugation on the microspin for 30 sec at 3 500 rpm.

The co-precipitation method was used to prepare nCa@2AT. For this 3 mL of aqueous solution polyacrylic acid (PAA, 3 mg/mL) was added to 3 mL of aqueous solution $CaCl_2$ (0.1M) and stirred for 1 h. Then, 100 μL of 2AT (0.5, 1, 2, 5 and 10 mg) were added to the mixture and stirred for 1 h. Then, 3 mL of aqueous solution Na_2CO_3 (0.1M) was added, and the mixture was stirred for 1 h. The final solution was washed 3 times with Milli-Q water and centrifuged for 4 min at 13 400 rpm.

4.2. 2AT drug loading efficiency

The solubility of 2AT was assessed in 3 media. For this purpose, 500 μL of H_2O pH 5.0, H_2O pH 7.0, and DMSO were added to 0.5 mg of 2AT. The best solubility was found in DMSO. To determine the 2AT concentration in the supernatants during loading and release experiments, calibration curves were constructed in PBS pH 7.4, HEPES pH 6.8, acetate buffer pH 5.0.

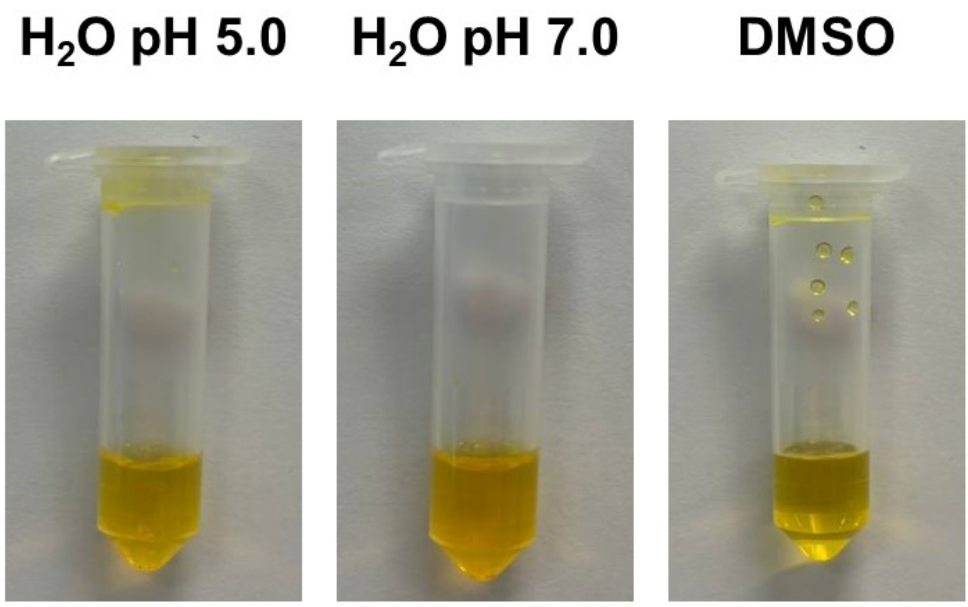

Fig. S6 Solubility of 2AT in various media: H_2O pH 5.0, H_2O pH 7.0, DMSO.

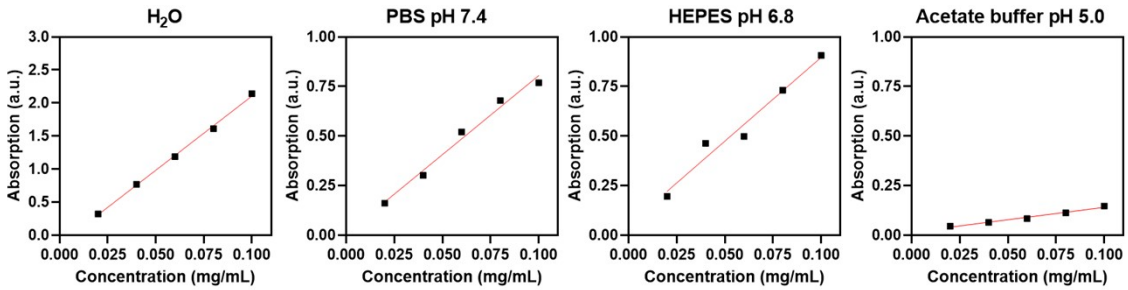

Fig. S7 Calibration curves of 2AT in different environments: H_2O, PBS pH 7.4, HEPES pH 6.8, acetate buffer pH 5.0, respectively.

Loading of 2AT into mCa and nCa was accomplished by co-precipitation in the water. Varying amounts of 2AT were loaded into the particles to evaluate the drug loading efficiency. After the first wash of mCa@2AT and nCa@2AT, the supernatants were collected, and the absorbance was measured at 423 nm. Then, the percentage of loaded 2AT (%) can be calculated as:

$$2\text{AT}\ (\%) = \frac{\text{amount of unloaded 2AT in supernatants (mg)}}{\text{amount of added 2AT (mg)}} * 100\%$$

5. ‘Cold’ labeling and ‘hot’ labeling

5.1. ‘Cold’ labeling of mCa@2AT and nCa@2AT

The ‘cold’ labeling of mCa@2AT and nCa@2AT (the radiolabeling procedure excluding the addition of radioactive isotope) was performed according to previously developed and published protocol [3]. To do this, 1000 μL of $BaCl_2$ (0.008M) and 1000 μL of Na_2SO_4 (0.011M) were mixed and the resulting solution was added to mCa@2AT and nCa@2AT. The resulting suspensions were shaken for 1.5 h. The particles were then washed 3 times with Milli-Q water and left for further investigation. Energy-dispersive X-ray spectroscopy (EDX) and thermogravimetric analysis (TGA) were used to quantify the composition of the final "cold"-labeled particles.

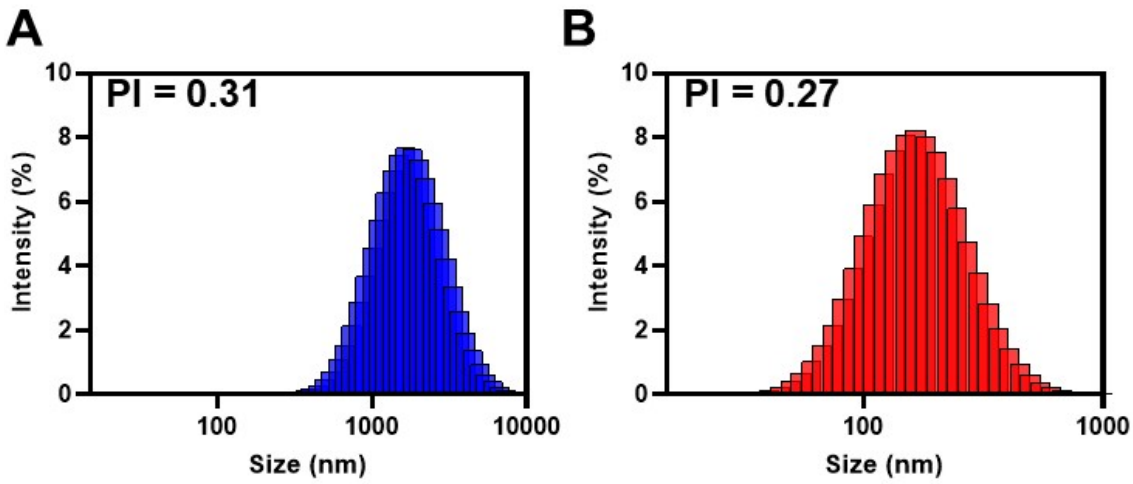

Fig. S8 A: D_h distribution of ‘cold’ mCa@2AT. **B:** D_h distribution of ‘cold’ nCa@2AT.

A

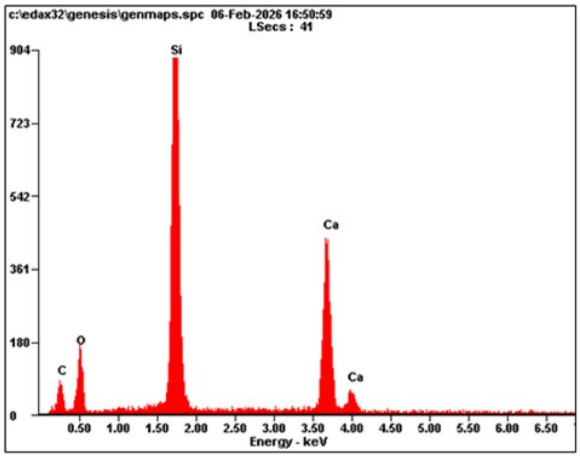

Element	Wt%	At%
CK	30.45	45.70
OK	25.71	28.97
SiK	29.25	18.77
CaK	14.58	06.56
Matrix	Correction	ZAF

B

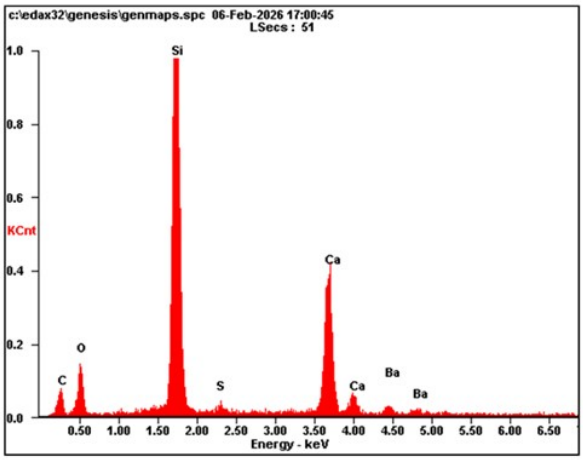

Element	Wt%	At%
CK	27.89	43.97
OK	23.00	27.22
SiK	32.27	21.76
SK	00.71	00.42
CaK	13.16	06.22
BaL	02.97	00.41
Matrix	Correction	ZAF

Fig. S9 A: EDX spectra of mCa. **B:** EDX spectra of 'cold' mCa.

5.2. 'Hot' labeling

The 'hot' labeling of mCa@2AT and nCa@2AT with radium-223 (^{223}Ra) isotope was performed using the 'cold' labeling protocol with an addition of radioactive isotope. To do this, 1000 μL of $BaCl_2$ (0.008M), 1000 μL of Na_2SO_4 (0.011M), and 100 μL of $^{223}Ra^{2+}$ solution (0.5 MBq) in 0.9% NaCl were mixed with mCa@2AT and nCa@2AT. The resulting suspensions were shaked for 1 h. The particles were then washed 3 times with Milli-Q water. The radiolabeling efficiency (%) was calculated by measuring the activity of the samples before the washing (start) and after each washing step.

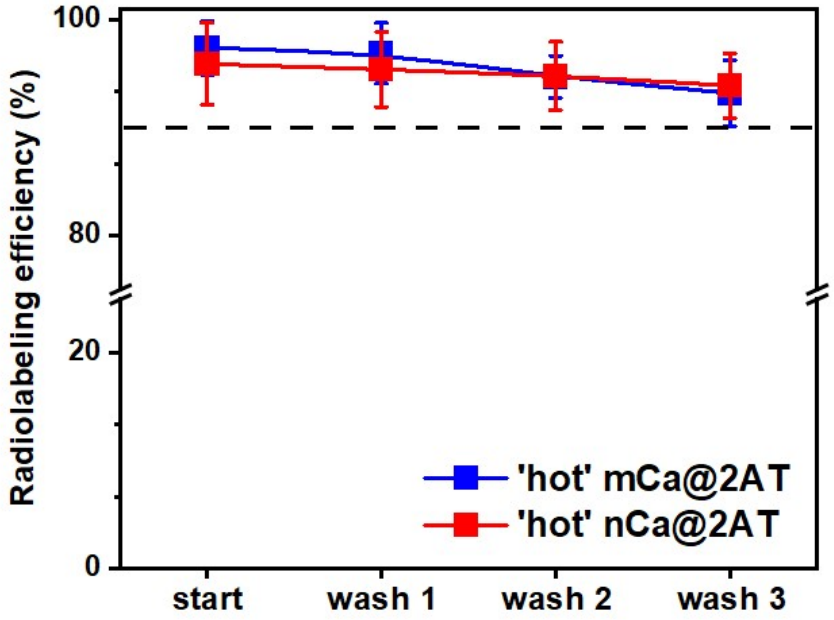

Fig. S10 Radiolabeling efficiency of 'hot' labeling of mCa@2AT and nCa@2AT. The results are presented as mean ± standard deviation (n = 3).

5.3. Synthesis of 'cold' mCa@Cy5 and 'cold' nCa@Cy5 particles

The co-precipitation method was used to prepare mCa@Cy5. For this 300 μL of Cy5-BSA were added to 2.2 mL of Milli-Q water. Then 615 μL of aqueous solution of $CaCl_2$ (0.1M) and 615 μL of aqueous solution of Na_2CO_3 (0.1M) were added to the first solution. The resulting suspension was stirred for 30 sec and centrifuged on the microspin for 30 sec at 3 500 rpm.

The co-precipitation method was used to prepare nCa@Cy5. For this 300 μL of Cy5-BSA was added to 3 mL of aqueous solution $CaCl_2$ (0.1M) and stirred for 1 h. Then, aqueous solution polyacrylamide (PAA, 3 mg/mL) was added to the solution and left to mix for 1 h. Then, 3 mL of aqueous solution Na_2CO_3 (0.1M) was added, and the mixture was stirred for 1 h. The final solution was washed 3 times with Milli-Q water and centrifuged for 4 min at 13 400 rpm.

6. *In vitro* stability

Using the dynamic light scattering method, information on the stability of all particles (mCa, nCa, mCa@2AT, nCa@2AT, 'cold' mCa@2AT, 'cold' nCa@2AT) was obtained. The particles were incubated in 0.9% NaCl at pH 7.4. At certain time intervals (1, 24, 48, 72, 96 h), particle size was measured using a DLS Nano Particle Analyzer, Jinan Winner Particle Instrument Stock Co. (China). The solubility of mCa was tested in acetate buffer pH 5.

`

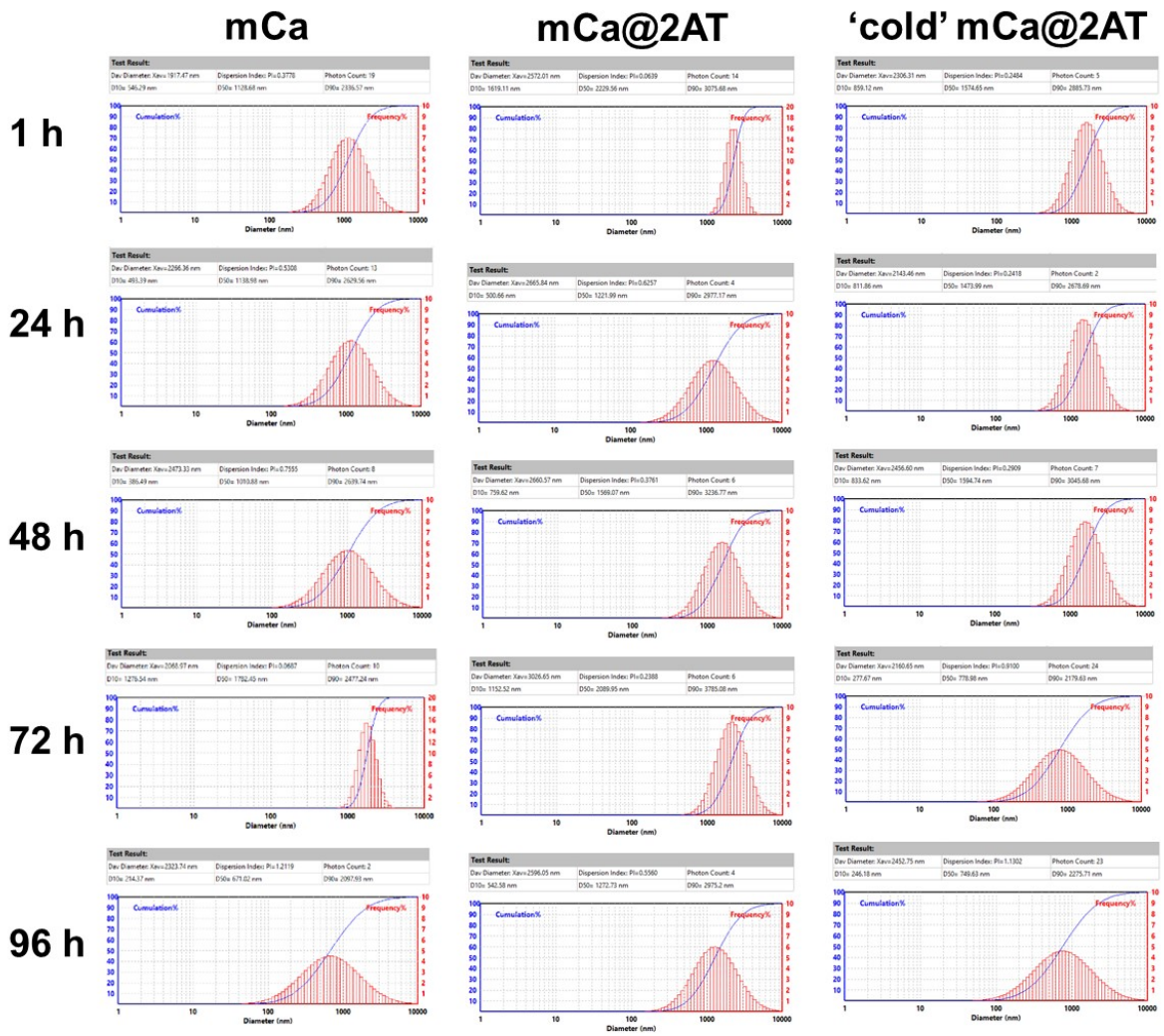

Fig. S11 Hydrodynamic diameters (D_h) of mCa, mCa@2AT, 'cold' mCa@2AT incubated in 0.9% NaCl at pH 7.4 during 96 h.

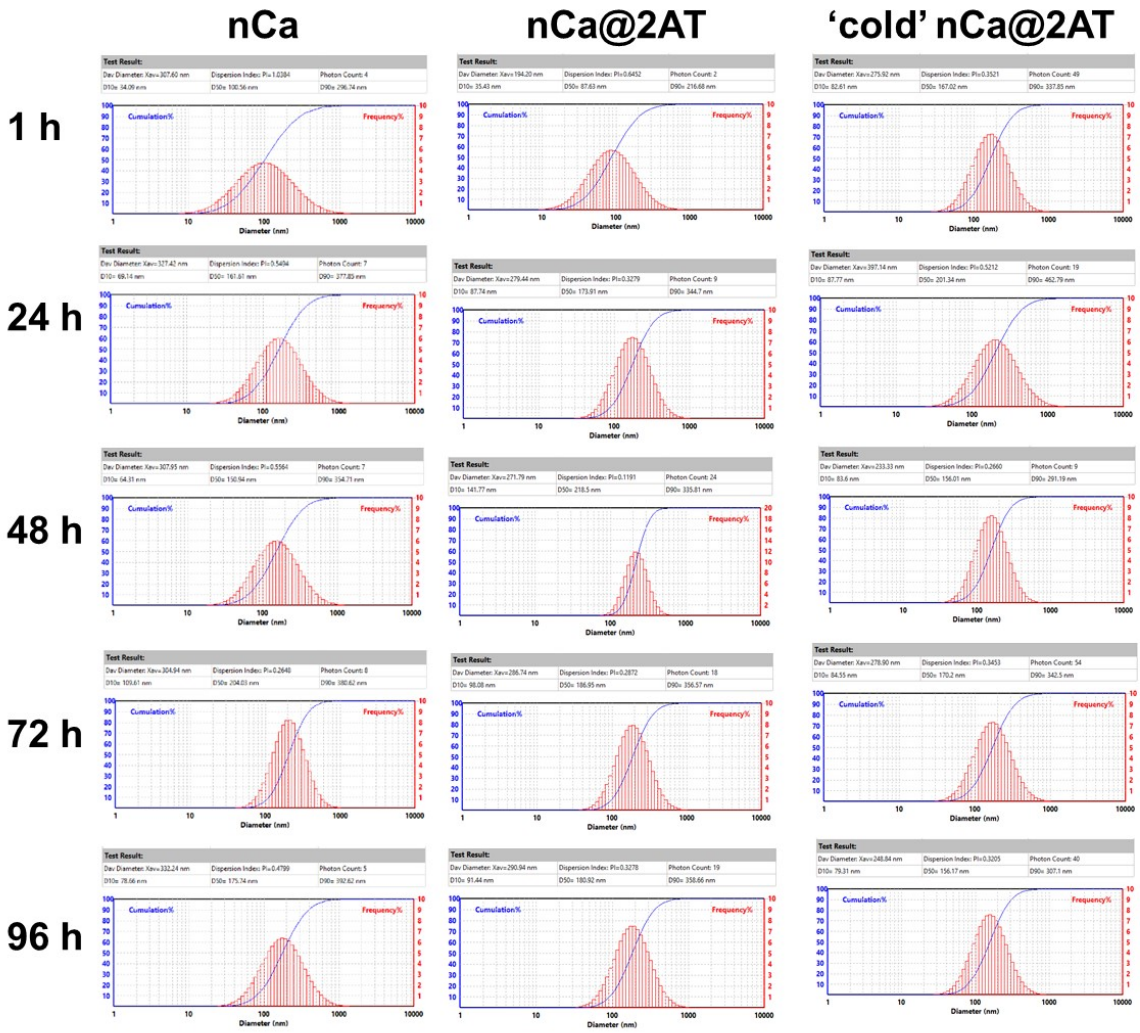

Fig. S12 Hydrodynamic diameters (D_h) of nCa, nCa@2AT, 'cold' nCa@2AT incubated in 0.9% NaCl at pH 7.4 during 96 h.

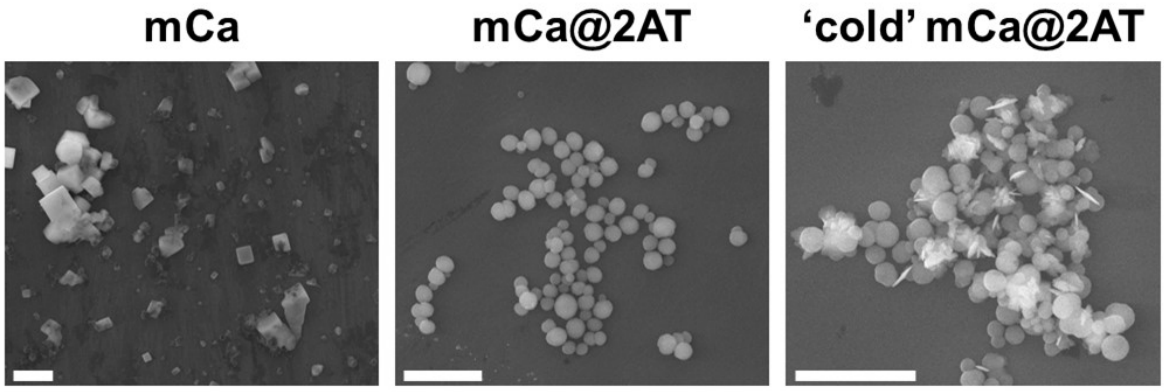

Fig. S13 SEM images of particles after 96 h of incubation in 0.9% NaCl pH 7.4. Scale bars correspond to 12 μm.

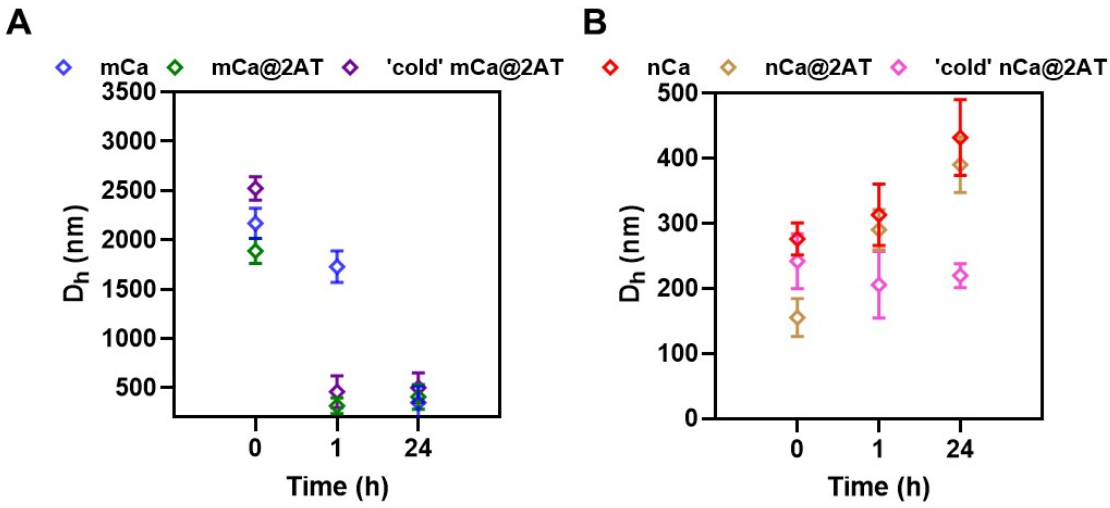

Fig. S14 Stability of mCa, mCa@2AT and 'cold' mCa@2AT in acetate buffer pH 5.0.

7. *In vitro* studies

7.1. In vitro investigation of mCa, nCa, 'cold' mCa, 'cold' nCa

7.1.1. Uptake study

The uptake assay was used to determine the quality of particle penetration into the cells. First, B16-F10 cells were seeded into a 6-well plate at a density of 25×10^4 cells per well. The plate was incubated for 24 h at 37°C and 5% CO_2. After the cells had attached to the plate surface, 'cold' mCa@Cy5 and 'cold' nCa@Cy5 were added to each well at five concentrations (0.25, 0.50, 1.00, 2.00, 3.00 mg/mL). After 24 h of incubation, the preparatory stage began. The culture medium was removed from the wells, and the cells were washed twice with PBS. The cells were then fixed with 10% formalin for 1 h and washed again. Staining step: 40 μL of doxorubicin was added to each well to stain cell nuclei. After 24 h the cells were washed in PBS and TWEEN80 (100 μL in 2 mL PBS) was added at a volume of 80 μL per well. The plate was left for 10 min, then the cells were washed with PBS, and FITC-phalloidin (100 μL in 2 mL of PBS) was added at a volume of 150 μL per well to stain the cell cytoplasm. The plate was left in the

refrigerator overnight, then the cells were washed again in PBS and examined on a confocal laser scanning microscope (Leica TCS SP8 (Germany)). The confocal pinhole was set to 1 Airy unit, and the images were taken with an HC PL FLUOTAR 10x/0.30 PH2 Objective.

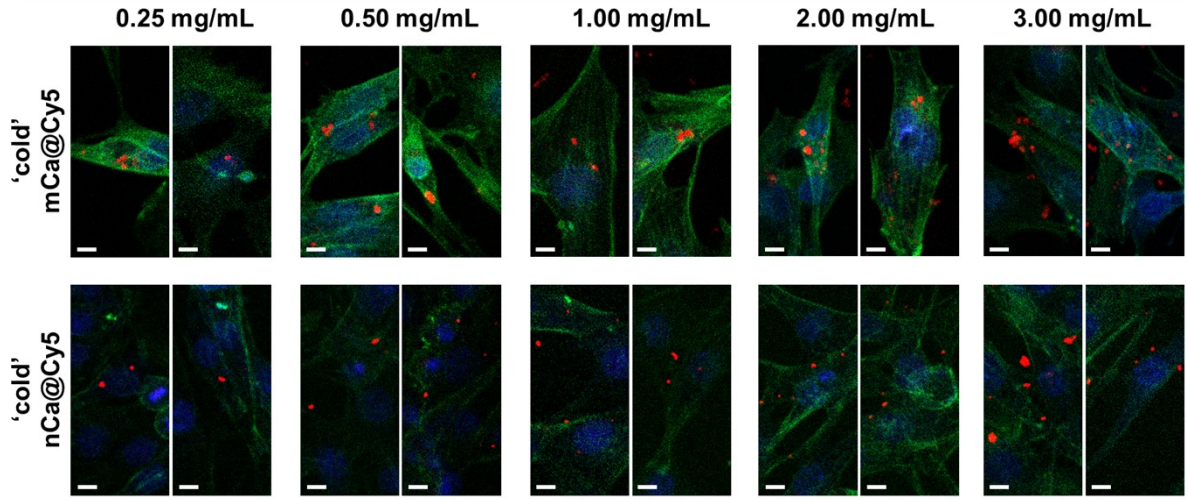

Fig. S15 CLSM images of B16-F10 cells after 24 h incubation with 'cold' mCa@Cy5 and 'cold' nCa@Cy5. Scale bars correspond to 10 μm.

7.1.2. Colocalisation study with LysoTracker Green

For colocalisation assay B16-F10 cells were seeded into 6-well plates at a density of 25 × 10^4 cells per well. The plate was incubated for 24 h at 37°C and 5% CO_2. After cell attachment, 'cold' mCa@Cy5 and 'cold' nCa@Cy5 were added to the cells at a concentration of 3.00 mg/mL. The cells were further incubated for 24 h under the same conditions. After incubation, the cells were washed twice with PBS. LysoTracker Green was then added according to the manufacturer's instructions and incubated with the cells for 30 min at 37 °C to stain lysosomes. After staining, the cells were washed with PBS to remove excess dye. The cells were subsequently fixed with 10% formalin for 1 h at room temperature and washed again with PBS. The plate was left in the refrigerator overnight, then the cells were washed again in PBS and examined on a confocal laser scanning microscope (Leica TCS SP8 (Germany)). The confocal pinhole

was set to 1 Airy unit, and the images were taken with an HC PL FLUOTAR 10x/0.30 PH2 Objective.

7.1.3. Flow cytometry

The cellular uptake of 'cold' mCa@Cy5 and 'cold' nCa@Cy5 was investigated using flow cytometry. To do this, B16-F10 cells were seeded on a 6-well plate (5×10^5 cells per well), which was then incubated for 24 h at 37°C and 5% CO_2. The next day, 'cold' mCa@Cy5 and 'cold' nCa@Cy5 were added to the cells at different concentrations: 1, 4, and 6 mg/mL. The cells with the particles were incubated for 24 h to ensure adequate absorption of the samples. After incubation, the cells were carefully removed from the plate, washed with PBS, and then left in 1 mL of PBS for subsequent analysis. The absorption analysis was conducted using flow cytometry (Cytek Northern Lights, USA), which allowed for a detailed examination of the level of the particles' absorption by the cells.

7.1.4. AlamarBlue assay

To determine the particle toxicity level on cells, the AlamarBlue test was conducted. The toxicity of mCa, nCa, 'cold' mCa, 'cold' nCa was tested on the B16-F10 (melanoma) and MDCK (madin-darby canine kidney) cell lines. For this purpose, 1 million cells were seeded into a 96-well plate (1×10^4 cells per well), which was then incubated for 24 h at 37°C and 5% CO_2. Particles were then added to the plate at various concentrations (0.006 – 3.000 mg/mL). After 24 h the culture medium was removed and the resazurin dye (10% v/v) was added to each well. After 4 h the absorbance was analyzed using a ELISA Microplate Reader at two wavelengths: 570 and 600 nm to determine the cell viability.

The results were evaluated according to the formula:

$$\text{Cell viability (\%)} = \frac{(O2 \times A1) - (O1 \times A2)}{(O2 \times P1) - (O1 \times P2)} \times 100\%,$$

where:

O1 = molar extinction coefficient (E) of the oxidized alamarBlue at 570 nm (80586);

O2 = E of the oxidized alamarBlue at 600 nm (117216);

A1 = absorbance of the test wells at 570 nm;

A2 = absorbance of the test wells at 600 nm;

P1 = absorbance of the positive growth control wells (cells plus alamarBlue but no test agent) at 570 nm;

P2 = absorbance of the positive growth control wells (cells plus alamarBlue but no test agent) at 600 nm.

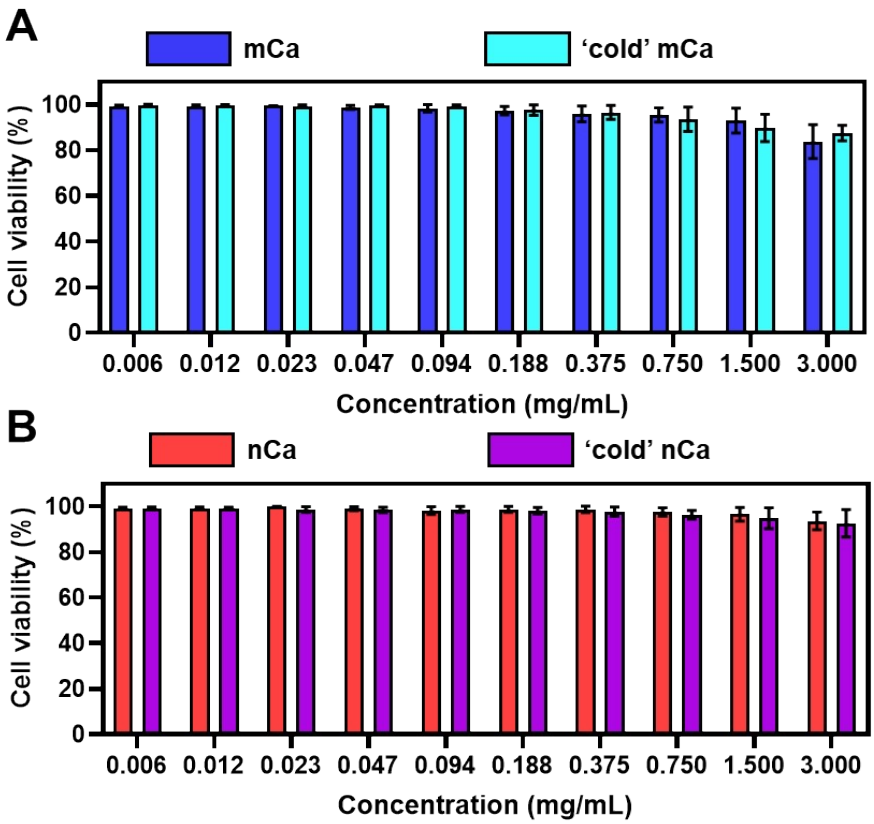

Fig. S16 A, B: Cell viability of MDCK cells after incubation with mCa, 'cold' mCa, nCa, and 'cold' nCa (0.006 – 3.000 mg/mL).

7.1.5. Hemolysis assay

The hemolysis assay was used to analyze the particle ('cold' mCa and 'cold' nCa) toxicity on the human red blood cells (RBCs). 3 mL of human blood

were added to 3 mL of Ficoll, the resulting solution was centrifuged for 20 min at 312 g. The precipitated RBCs were washed 3 times with PBS. The RBCs were then diluted to a final concentration (5% v/v) using PBS. The particles were added to the RBCs at various concentrations (0.5, 1.0, 2.0, 3.0 mg/mL). The RBCs diluted with PBS were used as a negative control, and a sample diluted with PBS and subjected to a 3-fold freeze-thaw procedure to release hemoglobin from the RBCs was used as a positive control. Using PBS, the final volume of the solutions was brought to 1 mL. The particles were incubated with the erythrocytes for 2 h, and then the samples were centrifuged for 5 min at 300 g. The percentage of hemolysis was calculated using the formula:

$$Hemolysis = \frac{OD\ (sample)\ -\ OD\ (negative\ control)}{OD\ (positive\ control)\ -\ OD\ (negative\ control)} \times 100\%,$$

where: OD - optical density.

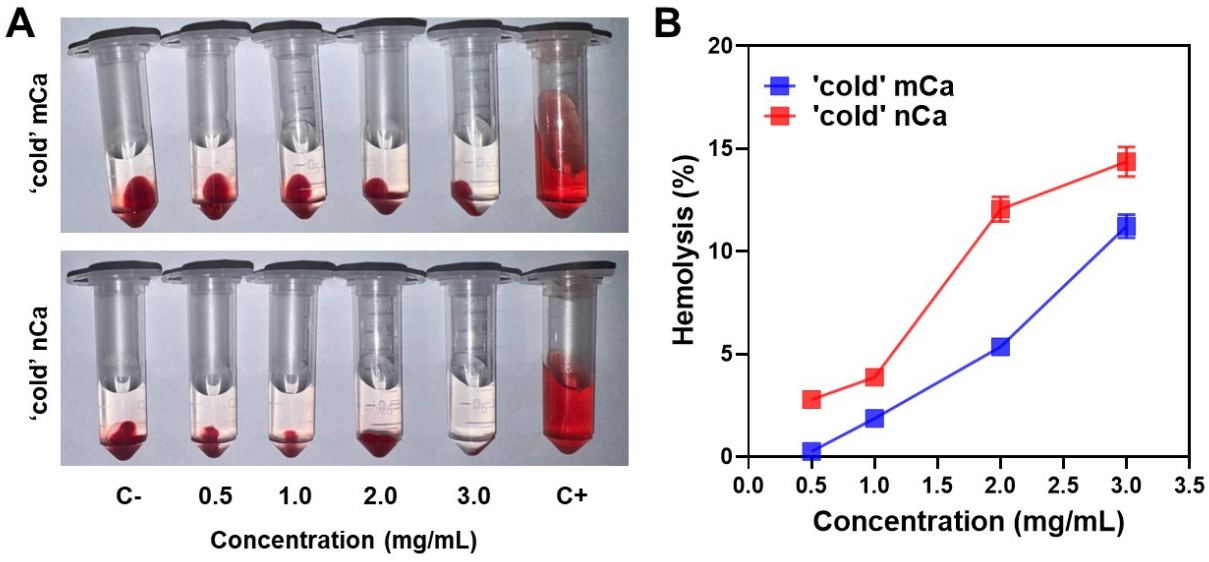

Fig. S17 A: Representative images of hemolysis assays, showing RBCs sedimentation and hemoglobin release. C- and C+ correspond to the negative and positive controls. **B:** Hemolysis assay graphs. The results are shown as an average value ± standard deviation (n = 3).

7.2. In vitro investigation of 'cold' mCa@2AT and 'cold' nCa@2AT

7.2.1. 2AT release efficiency

The release of 2AT from mCa@2AT, nCa@2AT, 'cold' mCa@2AT and 'cold' nCa@2AT was assessed in two solutions: acetate buffer at pH 5.0, HEPES at pH 6.8, 0.9% NaCl at pH 7.4. The packed mass of 2AT was 10 mg. At certain time intervals (1, 24, 48, 120, 144, 168 h) the particles were centrifuged, the supernatants were collected, and the absorbance was measured at 423 nm. After this, the particles were filled with new solutions and left to incubate until the next point. Knowing the calibration curve for 2AT, the drug release was calculated using the following formula:

$$\text{Cumulative release ratio (\%)} = \sum_{\text{time point}} \frac{m(released)}{m(loaded)} \times 100\%,$$

where *m(released)* - mass of released drug in supernatant, *m(loaded)* - mass of loaded drug. The detailed analysis of the kinetics of 2AT release from carriers was performed using the Higuchi, zero-order, and Karmayer-Peppas models.

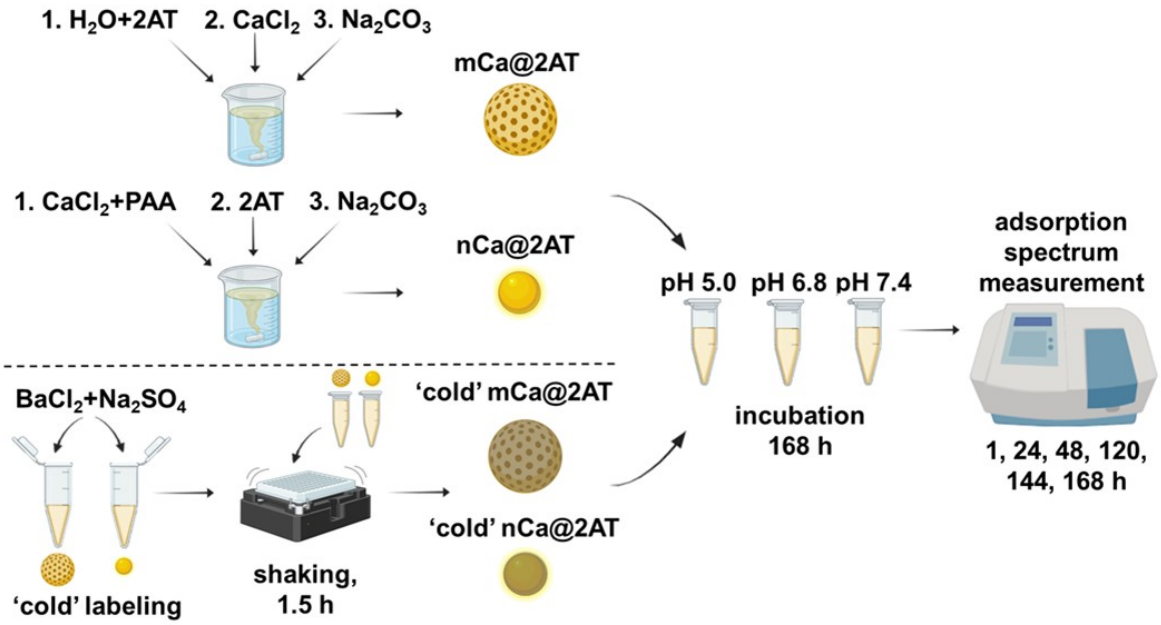

Fig. S18 Scheme of drug release studies.

Table S1 Values of R^2 and n for each type of particles.

Type of particles	Model Higuchi, R^2	Zero-order model, R^2	Model Korsmeyer-Peppas, R^2	Model Korsmeyer-Peppas, n	Mechanism of Drug Release
nCa@2AT pH 5.0	0.9205	0.8254	0.967	0.5932	Non-Fickian release
nCa@2AT pH 6.8	0.5859	0.45	0.8402	0.5976	Non-Fickian release
nCa@2AT pH 7.4	0.7434	0.6075	0.9114	1.111	Erosion
mCa@2AT pH 5.0	0.9136	0.8175	0.9969	0.724	Non-Fickian release
mCa@2AT pH 6.8	0.6857	0.5555	0.8606	0.4542	Fickian release
mCa@2AT pH 7.4	0.8255	0.7047	0.9583	0.2126	Fickian release
'cold' nCa@2AT pH 5.0	0.7553	0.628	0.8801	0.8697	Non-Fickian release
'cold' nCa@2AT pH 6.8	0.5668	0.4308	0.8348	0.6358	Non-Fickian release
'cold' nCa@2AT pH 7.4	0.8853	0.7766	0.955	1.412	Erosion
'cold' mCa@2AT pH 5.0	0.8563	0.7409	0.9773	0.7906	Non-Fickian release
'cold' mCa@2AT pH 6.8	0.7194	0.5872	0.9102	0.2067	Fickian release
'cold' mCa@2AT pH 7.4	0.7237	0.5863	0.9424	0.3882	Fickian release

7.2.2. AlamarBlue assay of 'cold' mCa@2AT and 'cold' nCa@2AT

To determine the particle toxicity level on cells, the AlamarBlue test was conducted. The toxicity of 'cold' mCa@2AT**,** 'cold' nCa@2AT and 2AT was tested on the B16-F10 cell line. For this purpose, 1 million cells were seeded into a 96-well plate (1×10^4 cells per well), which was then incubated for 24 h at 37°C and 5% CO_2. Particles were then added to the plate at various concentrations (0.006 – 3.000 mg/mL). The amount of added 2AT varied in the range from 0.6 – 300.0 μg per well. After 24 h the culture medium was removed and the resazurin dye (10% v/v) was added to each well. After 4 h the absorbance was analyzed using a ELISA Microplate Reader at two wavelengths: 570 and 600 nm to determine the cell viability.

The results were evaluated according to the formula:

$$\text{Cell viability (\%)} = \frac{(O2 \times A1) - (O1 \times A2)}{(O2 \times P1) - (O1 \times P2)} \times 100\%,$$

where:

O1 = molar extinction coefficient (E) of the oxidized AlamarBlue at 570 nm (80586);

O2 = E of the oxidized AlamarBlue at 600 nm (117216);

A1 = absorbance of the test wells at 570 nm;

A2 = absorbance of the test wells at 600 nm;

P1 = absorbance of the positive growth control wells (cells plus AlamarBlue but no test agent) at 570 nm;

P2 = absorbance of the positive growth control wells (cells plus AlamarBlue but no test agent) at 600 nm.

8. Animals

Healthy mice of the C57BL/6 strain (female, age 8 weeks, weight 18 – 22 g, Rappolovo, St. Petersburg, Russia) were used for *in vivo* studies. All animal studies were approved by the relevant local authorities and were conducted in accordance with the guidelines for the care and maintenance of animals (European Convention for the Protection of Vertebrate Animals used for Experimental and other Scientific Purposes). Mice were maintained at 22 – 24°C and 40 – 60% humidity, under a 12 h light/dark cycle, in standardized cages with free access to food and water, starting at least 15 d before the start of the experiments.

9. Mice tumor model (B16-F10 melanoma)

The B16-F10 cell line was used to create a solid tumor (melanoma). The cells were cultured in α-MEM nutrient medium containing 10% adult bovine serum (ABS) at 37°C and CO_2 5%. During the exponential growth phase, cells were trypsinized and concentrated to 1×10^6 per 100 μL. Mice were inoculated with the cell suspension in a volume of 100 μL into the right hind limb. After 7 d, the mice were examined for the satisfactory tumor size (approximately 0.05 ± 0.01 cm^3) for further use in experiments.

10. *In vivo* biodistribution studies

To determine the spatiotemporal distribution of ‘cold’ mCa@Cy5 and ‘cold’ nCa@Cy5 within mice, a qualitative and quantitative analysis was conducted. The study was conducted on C57BL/6 mice bearing B16-F10 melanoma tumors. After 14^{th} d from the injection of tumor cells into mice, the mice were divided into 9 groups (n = 3):

1) control 1 h,
2) ‘cold’ mCa@Cy5 1 h,
3) ‘cold’ nCa@Cy5 1 h,
4) control 24 h,

5) ‘cold’ mCa@Cy5 24 h,

6) ‘cold’ nCa@Cy5 24 h,

7) control 48 h,

8) ‘cold’ mCa@Cy5 48 h,

9) ‘cold’ nCa@Cy5 48 h.

Mice were injected with ‘cold’ mCa@Cy5 and ‘cold’ nCa@Cy5 in a volume of 100 μL into the tumor at a concentration of 7 mg/mL. Each time point indicates the time of ‘cold’ mCa@Cy5 and ‘cold’ nCa@Cy5 administration before the mice were sacrificed. Mice were euthanized by cervical dislocation. At first, whole-body fluorescence bioimaging was performed using Fluor i In Vivo (NeoScience, South Korea) to assess the particle distribution within the mice's hind limbs, where the tumor was located. Secondly, organs (lungs, heart, liver, spleen, kidneys) and tumors were removed from animals for the biodistribution of the particles, as well as the quantitative analysis. The Integrated Density (Area × Intensity Units) of each animal was detected by Fluor i In Vivo with the selected settings in a specific area.

Quantification of fluorescence intensity within organs and tumors *ex vivo* was performed by summing the fluorescence intensity (arbitrary intensity units) measured for each organ within each experimental group. The total fluorescence signal for a given group was defined as 100%, and the contribution of each individual organ was then recalculated as a percentage of this total as the relative distribution of fluorescence across the organs.

$$Fluorescence\ in\ organ\ (Flu, \%) = \frac{Intensity\ Unit_{organ}}{\sum Intensity\ Unit_{organs}} \times 100\ (\%)$$

In the case of the *in vivo* fluorescence biodistribution experiment over 96 h, the fluorescence intensity was calculated as follows: the method involves taking the fluorescence intensity at the first time point for each group as 100%.

Then, for all subsequent time points, the intensity is recalculated as a percentage of this value.

$$Fluoescence\ in\ tumor_n\ (Flu, \%) = \frac{Intensity\ Unit_n}{Intensity\ Unit_{1h}} \times 100\ (\%)$$

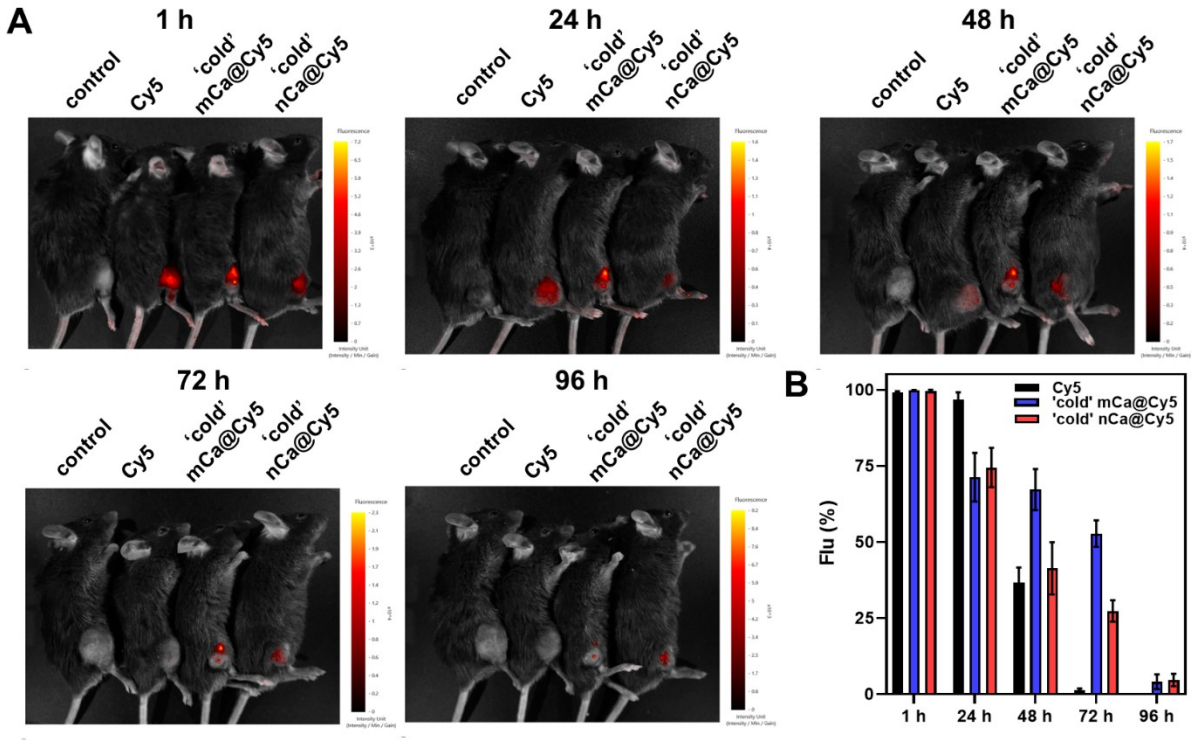

Fig. S19 A: Fluorescent images of the mice treated with 'cold' mCa@Cy5 and 'cold' nCa@Cy5 at 1, 24, 48, 72, 96 h of post-injection. **B:** Quantitative analysis of fluorescence signals from 'cold' mCa@Cy5 and 'cold' nCa@Cy5 in mice at 1, 24, 48, 72, 96 h of post-injection. The results are presented as mean ± standard deviation (n = 3).

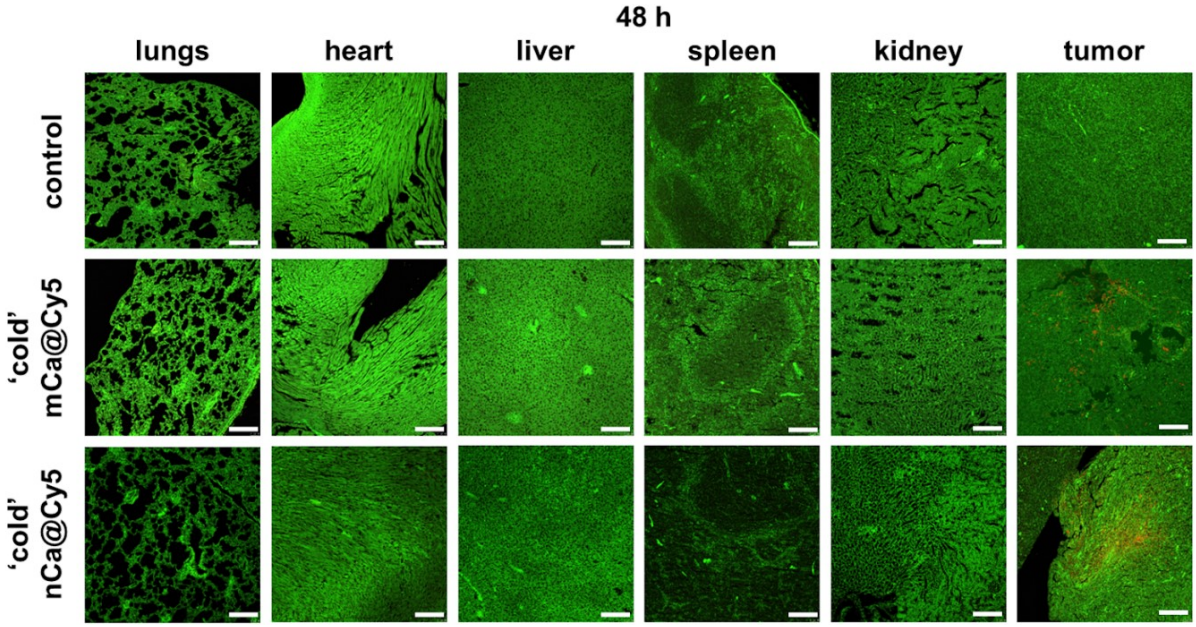

Fig. S20 Fluorescent images of H&E-stained tissues from the main organs (heart, lung, liver, spleen, and kidney) and tumors of mice 48 h after injection 'cold' mCa@Cy5 and 'cold' nCa@Cy5. Scale bars correspond to 150 μm.

11. Acute toxicity

The acute toxicity test was performed to assess long-term safety. On 0, 7th, and 14th d after the local injection, blood samples were taken from the animals for comprehensive biochemical analysis. The following indicators were used as diagnostic parameters for assessing the functional state of organs and systems: the levels of alanine aminotransferase (ALT), aspartate aminotransferase (AST), alkaline phosphatase (ALP), lactate dehydrogenase (LDH), creatinine (Crea), and blood urea nitrogen (BUN). The blood samples were put into the cartridge and analyzed using an automated biochemical analyzer (Vetliga (Russia)). In addition, the animals were weighed at specific times to assess their overall health and physiological stability: at the initial point (0 d), as well as on 2nd, 5th, 7th, 10th, and 15th d after the injection.

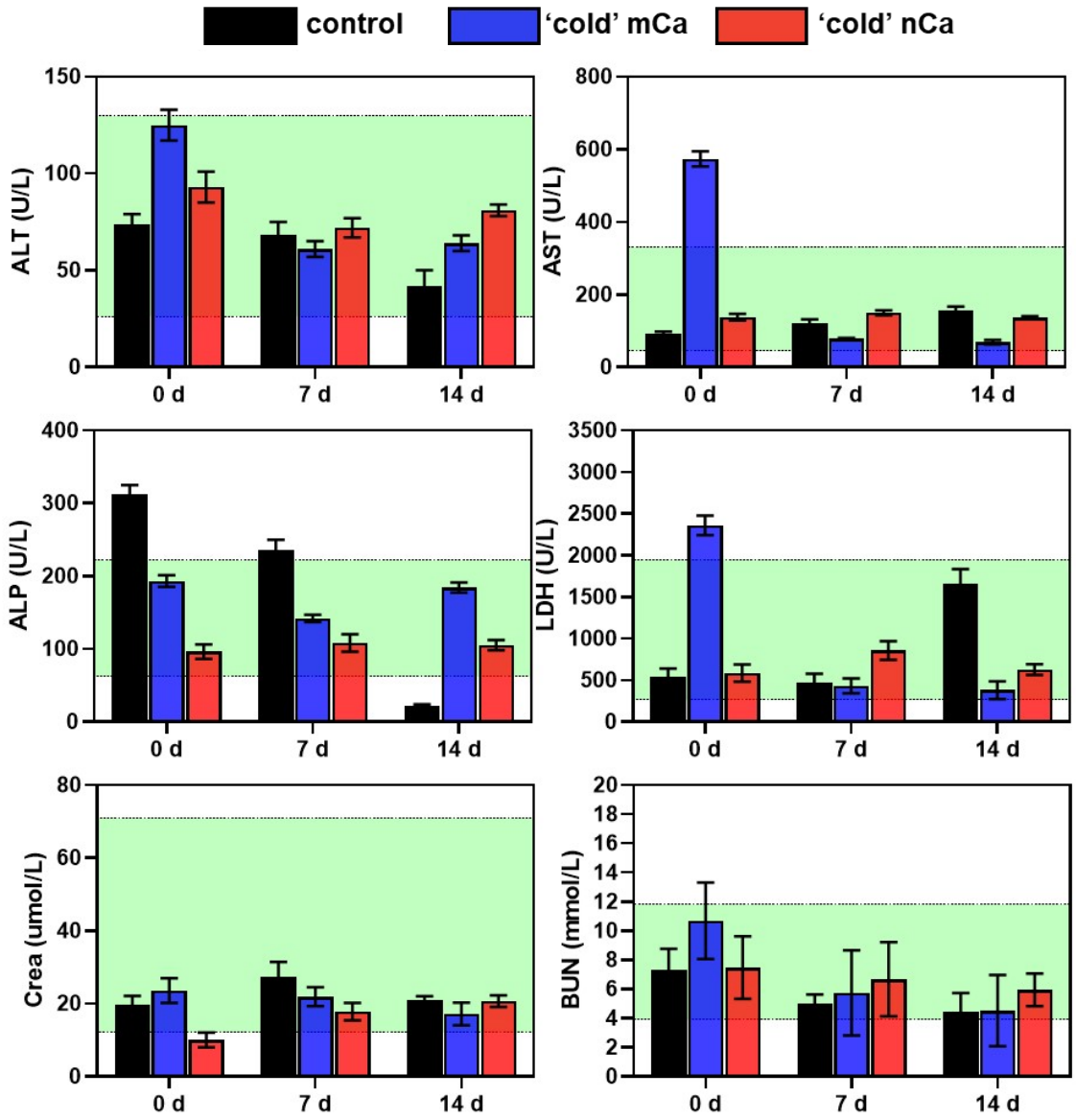

Fig. S21 Biochemical parameters (ALT, AST, ALP, LDH, Crea, and BUN) of C57BL/6 mice analyzed after local administration of 'cold' mCa and 'cold' nCa. The results are presented as mean ± standard deviation (n = 3).

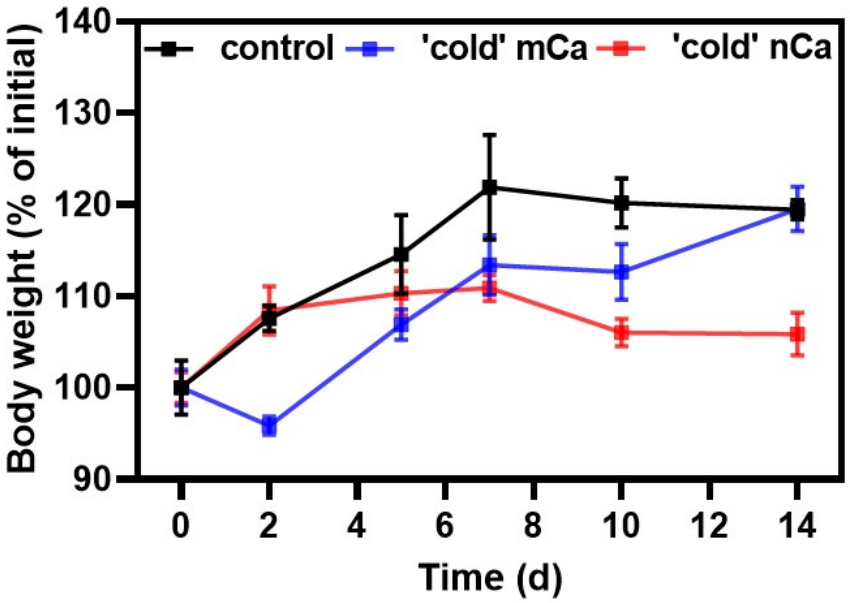

Fig. S22 Body weight monitoring of mice for 14 d.

12. *In vivo* therapeutic efficiency studies

The antitumor efficacy of 'cold' mCa@2AT and 'cold' nCa@2AT was investigated using C57BL/6 mice bearing tumors created by inoculation of B16-F10 melanoma cancer cells. Mice were inoculated with 100 μL of cell suspension (1×10^6 cells per 100 μL) in the right hind limb. On the 7th day after cell injection, the tumor volume reached ~50 mm^3, and therapy started. Mice were divided into 4 groups (n = 6):

1) control - mice not receiving treatment;

2) 'cold' mCa@2AT - mice treated with mCa (V = 50 μL, concentration 135 mg/mL) with encapsulated 2AT at a dose of 0.4 g per 1 kg of mice;

3) 'cold' nCa@2AT - mice treated with nCa (V = 50 μL, concentration 132 mg/mL) with encapsulated 2AT at a dose of 0.4 g per 1 kg of mice;

4) 2AT – mice treated with 2AT (50 μL of 2AT suspension, 120 mg/mL) at a dose of 0.4 g per 1 kg of mice.

Mice in the control group were not treated and were used for comparison with the treatment groups. On 1st, 3rd, 5th and 7th d, the mice were photographed

and weighed to monitor tumor reduction and assess their health, and the change in tumor volume was measured using a caliper. On 7 d, mice were euthanized by cervical dislocation, organs (lungs, heart, liver, kidneys and spleen) and tumors were removed for further histological analysis. The tumor volume (determined in cm^3) was calculated as $V=L\times W^2/2$ using a caliper, where L – tumor length and W – tumor width.

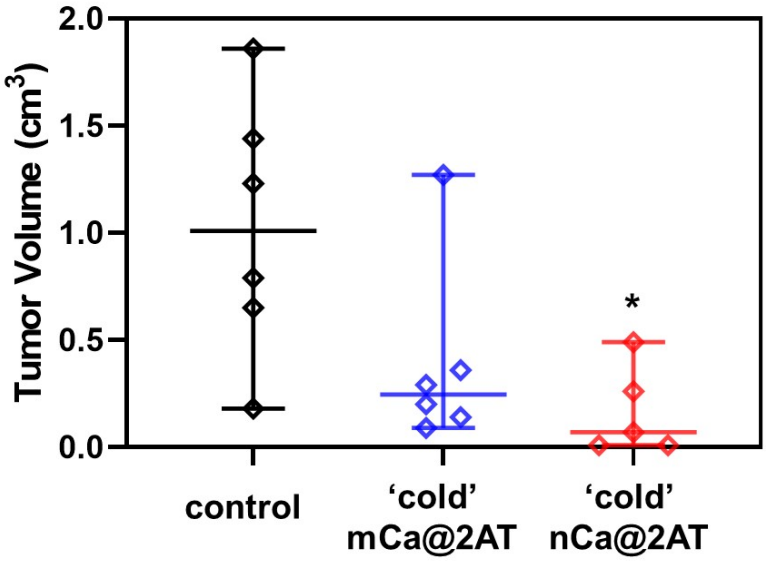

Fig. S23 Tumors' volume estimation after 7 d of therapy. The results are presented as mean ± standard deviation (n = 6). Symbol * represents $p < 0.05$.

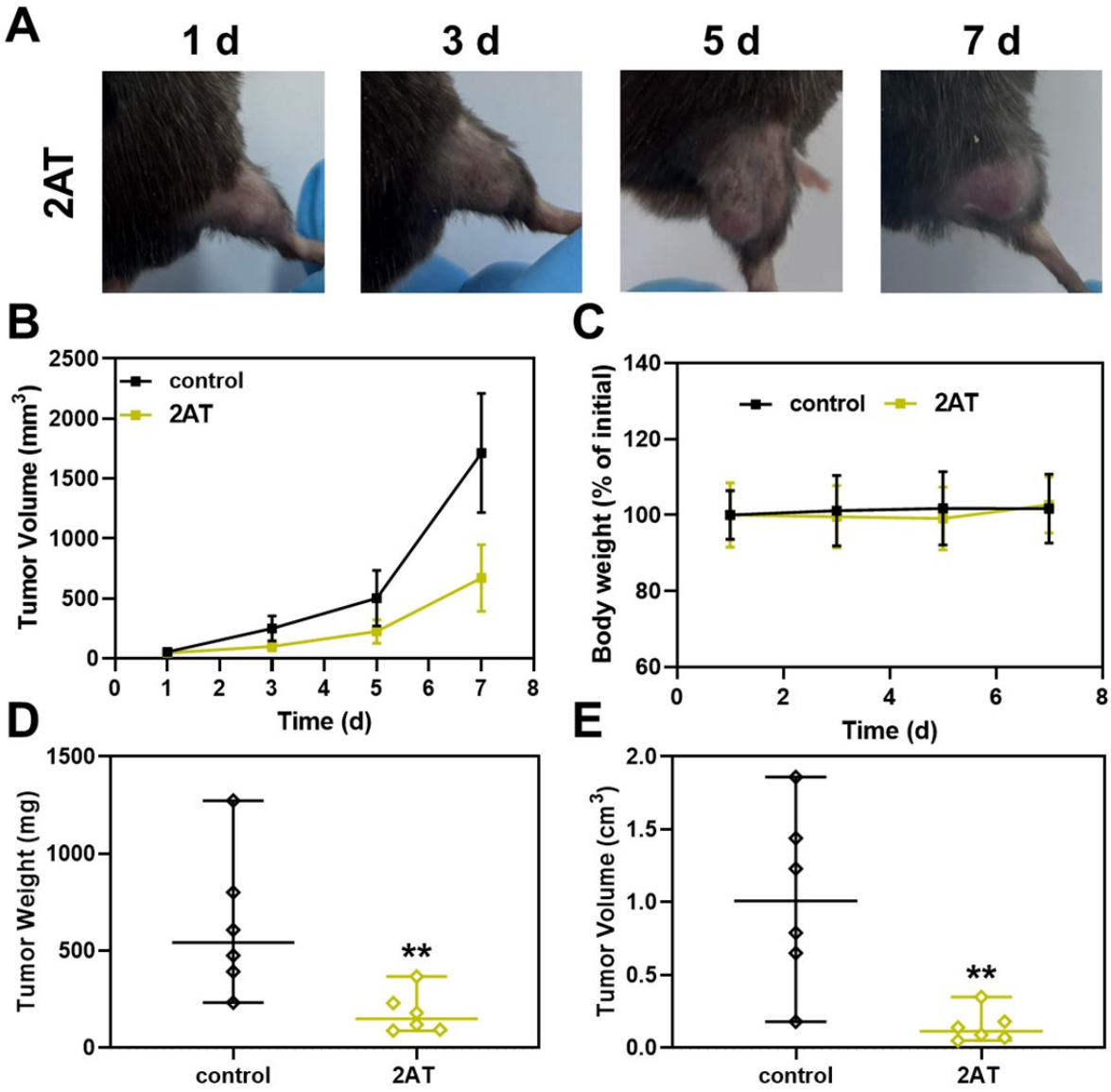

Fig. S24 A: Representative images of tumor progression in live mice during treatment on day 1, 3, 5 and 7 d. **B:** Tumor volume monitoring of mice for 7 d. **C:** Body weight monitoring of mice for 7 d. **D:** Tumors' weight estimation after 7 d of therapy. The results are presented as mean ± standard deviation (n = 6). Symbol ** represents $p < 0.01$. **E:** Tumors' volume estimation after 7 d of therapy. The results are presented as mean ± standard deviation (n = 6). Symbol ** represents $p < 0.01$.

13. Histological analysis

Histological preparations (lungs, heart, liver, kidneys, spleen and tumors) were prepared as follows. Dehydration and paraffin impregnation were performed using a standardized method in a Donatello automated histological processor (DiaPath, Italy) using IsoPREP ready-to-use solution (Biovitrum, Russia) and HISTOMIX paraffin medium (Biovitrum, Russia). Filling into paraffin blocks was carried out at a paraffin filling station using metal molds. Using a rotary microtome HM 325 (Thermo, USA), histological preparations with 2-3 μm thick organ sections were prepared (one histological preparation per cassette). Histological preparations were stained using the generally accepted standardized method of hematoxylin and eosin in accordance with the manufacturer's recommendations (Biovitrum, Russia). The preparations were scanned using the KFbio MagScanner KF-PRO-400 scanner, with an image archive created using the automated K-Viewer software.

Histological analysis was performed on hematoxylin and eosin–stained sections of major organs (lungs, heart, liver, spleen, and kidney). Sections were coded and evaluated in a blinded manner by an independent investigator (Table S2). A semi-quantitative scoring system (0–3) was used to assess inflammatory infiltration and tissue damage/necrosis. Scores were assigned based on the severity and extent of pathological changes and averaged across multiple randomly selected fields per section.

Table S2 Semi-quantitative histopathological scoring system

Score	Inflammation	Necrosis / tissue damage	Organ architecture
0	No inflammatory cells	No necrosis or cellular damage	Normal architecture
1	Minimal inflammatory cell infiltration (scattered cells)	Mild, focal cellular damage	Slight, focal architectural alteration
2	Moderate inflammatory infiltration (localized clusters)	Moderate tissue damage	Noticeable but limited architectural disruption
3	Severe, diffuse inflammatory infiltration	Extensive necrosis or tissue damage	Severe, widespread architectural disruption

References

1 A. Rogova, I. A. Gorbunova, T. E. Karpov, R. Y. Sidorov, A. E. Rubtsov, D. A. Shipilovskikh, A. R. Muslimov, M. V. Zyuzin, A. S. Timin and S. A. Shipilovskikh, *Eur. J. Med. Chem.*, 2023, **254**, 115325.

2 Y. Kenzhebayeva, I. Gorbunova, A. Dolgopolov, M. V. Dmitriev, T. Sh. Atabaev, E. A. Stepanidenko, A. S. Efimova, A. S. Novikov, S. Shipilovskikh and V. A. Milichko, *Adv. Photonics Res.*, DOI:10.1002/adpr.202300173.

3 D. R. Akhmetova, K. A. Mitusova, A. S. Postovalova, A. S. Ivkina, A. R. Muslimov, M. V. Zyuzin, S. A. Shipilovskikh and A. S. Timin, *Biomater. Sci.*, 2024, **12**, 453–467.